International Journal for Housing Science and Its Applications
Publish August 10, 2025. Volume 46, Issue 4 Pages 7986-7996

https://doi.org/10.70517/ijhsa464684

Smart photovoltaic power station gray wolf optimization algorithm-driven component efficiency improvement

Shaoping Zhou[1], Yikun Cao[1,*] and Xiang Li[1]
[1] Chengdu Engineering Corporation Limited, Power China, Chengdu, Sichuan, 611130, China
Corresponding authors: (e-mail: 13608026304@163.com).

Abstract Big data computing and other technologies can improve the effectiveness of photovoltaic power plant management optimization. This paper uses the traditional gray wolf optimization (GWO) algorithm to optimize and extract the five parameters of the single diode model of photovoltaic components. Considering the objective function of purchase cost and cost loss, the paper seeks the possibility of achieving the optimal configuration with the lowest total cost. A spatial recognition mechanism is introduced to optimize the gray wolf algorithm, and the degree of violation of multi-step calculation time constraints is calculated to iteratively complete the global solution through local optimization breakthroughs. Research shows: The Gray Wolf optimization algorithm achieved a 100.0% success rate in optimization across five test functions. The optimized power generation cost was only 1.20270×10^4 yuan, and the optimal solution was obtained after 118 iterations. The improvement in photovoltaic power generation reached up to 51.5%, with voltage fluctuations under different operating conditions less than 0.01V, achieving efficient and stable power generation.

Index Terms photovoltaic module model, gray wolf optimization algorithm, parameter extraction, spatial identification mechanism, constraint violation degree.

I. Introduction

Photovoltaic power plants utilize the photovoltaic effect of solar energy to directly convert solar radiation into electrical energy. As a key component of the renewable energy sector, they are increasingly playing a significant role in the global energy structure [1]-[3]. Photovoltaic power plants primarily consist of photovoltaic modules, combiner boxes, inverters, box-type transformers, and monitoring systems [4], [5]. Photovoltaic modules are the core power-generating units of the power plant, composed of multiple photovoltaic cells connected in series and parallel. They are responsible for converting solar energy into direct current. During operation, photovoltaic modules are subjected to atmospheric pollution, dust, and dew, which severely impact the efficiency and reliability of photovoltaic power plants [6]-[9]. Therefore, improving module efficiency is crucial for ensuring the normal operation and long-term reliability of photovoltaic power plants, and intelligent management provides the technical support to achieve this goal [10], [11].

Based on current practical experience in the operation and management of photovoltaic power plants, to ensure the safe, economical, and efficient operation of photovoltaic power generation systems, it is particularly important to adopt an integrated photovoltaic power plant intelligent management strategy that combines real-time monitoring, centralized management, intelligent early warning analysis, and disaster prevention to establish standardized and effective management mechanisms, especially to ensure efficient operation and maintenance management [12]-[15]. Through data collection and transmission, information storage and processing, and intelligent analysis and prediction, intelligent management of photovoltaic power plants enables plant managers to more accurately predict potential events in plant operations and management, more promptly allocate resources, and take timely and effective measures for mitigation, prevention, and resolution, thereby maintaining the effective operation and management of photovoltaic power plants [16]-[19]. In this context, intelligent algorithms can be utilized to enhance the efficiency of power plant components. The Gray Wolf optimization algorithm, as an emerging optimization algorithm, exhibits significant optimization effects in complex and dynamic environments. By optimizing the parameter configuration, model prediction, and control strategies of the power plant system, it can enhance the efficiency of photovoltaic power plant components, thereby ensuring the efficiency, safety, and reliability of photovoltaic power plants [20]-[23].

Reference [24] proposes an IoT-based solar photovoltaic monitoring, maintenance, and management model, constructs a mathematical model for solar photovoltaics and its implementation algorithm, and designs an embedded expert system as a proof of concept, demonstrating the system's effectiveness in fault identification, classification, and analysis while ensuring data integrity. Reference [25] identifies the challenges currently faced in smart grid management, reviews theoretical prediction methods for solar resources and photovoltaic power generation, and explores the application of solar prediction in smart grid management. Reference [26] develops a smart management system for photovoltaic panel equipment, which employs the YOLOv5 object detection model to identify and detect the number and anomalies of photovoltaic panels based on images, demonstrating advantages such as efficient intelligent management, high-precision identification, and comprehensive anomaly detection. Literature [27] proposes an IoT-based intelligent operation and maintenance system for distributed photovoltaic power plants, which can achieve real-time monitoring, fault prediction, performance optimization, and automated maintenance decision-making. Experiments have validated its effectiveness in improving the operational efficiency and stability of photovoltaic power plants. Literature [28] reviews the application of artificial intelligence and IoT technologies for autonomous monitoring and analysis of large-scale photovoltaic power plants, aiming to automate the photovoltaic system status monitoring process. Research indicates that the development of autonomous monitoring and analysis for photovoltaic power plants can enhance the efficiency and reliability of photovoltaic systems. The above studies examine the intelligent management of photovoltaic power plants, outlining its significant advantages in areas such as power plant safety monitoring and fault detection, while also revealing the challenges it currently faces.

Literature [29] introduces photovoltaic (PV) technology and its advantages, and examines the impact of changing operational parameters such as irradiance intensity, humidity, and dust on PV module performance. The results indicate that these factors all influence PV module performance. Literature [30] discusses the types of defects formed in photovoltaic panels and proposes a method to determine defects based on the temperature and output power of aged photovoltaic modules. The study ultimately verifies that this method effectively reduces output losses in solar power plants and improves the efficiency of photovoltaic power plants. Literature [31] introduces the application of meta-heuristic techniques such as Gray Wolf Optimization (GWO) under different conditions, proposes the optimal size of PV modules and inverters, as well as the optimal distribution of PV modules within inverters. Through comparison, it demonstrates that this method is highly effective in addressing PV power plant optimization design issues. Literature [32] proposes an improved Gray Wolf Optimization Algorithm (GWOA) aimed at achieving maximum power point tracking (MPPT) for photovoltaic module arrays. Simulation studies reveal the effectiveness of the improved GWOA algorithm, demonstrating excellent tracking speed response and steady-state response. Reference [33] proposes an optimization configuration method for PV intelligent edge terminals (IETs). Based on the economic and reliability aspects of PV IET optimization, a two-layer optimization model is constructed, and improved adaptive genetic algorithms and gray wolf optimization algorithms are proposed. The study demonstrates that the aforementioned optimization configuration methods ensure reliability and cost control. The above studies identify factors influencing the performance of photovoltaic power generation components, emphasize their impact on photovoltaic power generation efficiency, and highlight methods such as gray wolf optimization and improved gray wolf optimization algorithms that can enhance the performance, efficiency, and safety of photovoltaic power plants and components.

This paper focuses on the advantages of intelligent optimization algorithms in improving the configuration efficiency of photovoltaic power plant components. Through methods such as model construction and computational solution, it explores optimal configuration schemes. Based on a five-parameter model using a single diode, a mathematical model of photovoltaic modules is established, and the gray wolf algorithm is employed to extract and adjust optimal parameters. Investment costs and reliability cost losses are quantified, and the efficiency improvement problem is transformed into a target function for solution. To address multi-dimensional constraint relationships, a spatial identification mechanism is introduced to enhance the traditional gray wolf algorithm's ability to calculate constraint violation degrees during search. By improving the performance of global solution iteration comparison, the optimal efficiency improvement scheme for photovoltaic modules is identified.

II. Technology for improving the efficiency of photovoltaic power station components based on the gray wolf optimization algorithm

II. A. Research on Mathematical Models of Photovoltaic Modules

II. A. 1) Equivalent circuit model and internal parameters of photovoltaic modules

The equivalent circuit model of photovoltaic modules can be divided into single-diode models and double-diode models based on the number of diodes connected in parallel. Figure 1 shows the single-diode model of a photovoltaic module. Figure 2 shows the double-diode model of a photovoltaic module.

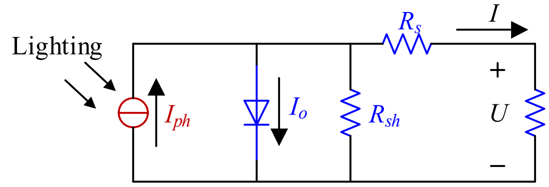

Figure 1: Single diode model of PV module

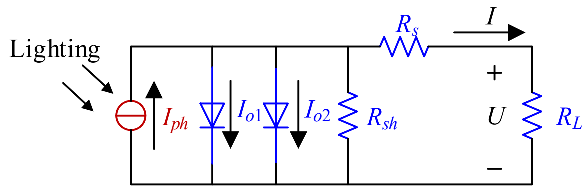

Figure 2: Double diode model of PV module

Among these, the single diode model has five internal parameters: photogenerated current I_{ph}, diode saturation reverse current I_o, diode quality factor A, equivalent parallel resistance R_{sh}, and equivalent series resistance R_s. Compared to the single diode model, the double diode model further accounts for the fact that the depletion region of a photovoltaic cell has some recombination current loss, and adds an additional equivalent diode in parallel to the single diode model, thereby achieving higher accuracy. However, since the dual-diode model includes an additional equivalent diode, it introduces two additional model parameters: the diode reverse saturation current I_{o2} and the diode quality factor A_2, resulting in a total of six model parameters. This makes the establishment of such a model more challenging and reduces computational efficiency.

Comparing and evaluating the two models, it was found that the single-diode model offers a better balance between model establishment difficulty and accuracy compared to the double-diode model, making it more suitable for theoretical analysis and engineering applications. Therefore, this paper establishes a mathematical model for photovoltaic modules based on the single-diode model (or five-parameter model).

Equation (1) is the UI characteristic equation of the single-diode five-parameter model:

$$I = I_{ph} - I_o \left\{ \exp\left[\frac{q\left(U + IR_s\right)}{ATK} \right] - 1 \right\} - \frac{U + IR_s}{R_{sh}} \tag{1}$$

In the equation, U is the component output voltage; I is the component output current; I_{ph} is the photocurrent; I_o is the diode reverse saturation current; A is the quality factor; R_s is the equivalent series resistance; R_{sh} is the equivalent parallel resistance; T is the absolute temperature of the component (K); K is the Boltzmann constant; q is the electron charge.

II. A. 2) Intelligent Optimization Algorithm

Intelligent optimization algorithms, such as the artificial fish school optimization algorithm, symbiotic biological search algorithm, artificial bee colony optimization algorithm, artificial neural network algorithm, and gray wolf optimization algorithm, have been incorporated into the extraction of five parameters and the establishment of a component model. Since intelligent optimization algorithms retain all parameters of the photovoltaic component single diode model during parameter extraction, avoiding accuracy loss caused by equation simplification, this method has significant advantages in terms of accuracy and reliability compared to the other three methods. However, most traditional intelligent optimization algorithms often suffer from issues such as getting stuck in local optima and excessive algorithm optimization time.

For the establishment of the mathematical model, the five-parameter values obtained under STC conditions are substituted into the empirical formulas varying with S and T (Equations (2)–(7)), and combined with the UI characteristic equations obtained using the Lambert W function decoupling method (Equations (8)–(9)), to establish the mathematical model of the photovoltaic module under any operating conditions:

$$I_{ph} = \frac{S}{S_{ref}} \left(I_{ph,ref} + \alpha \left(T - T_{ref} \right) \right) \tag{2}$$

$$I_o = I_{o,ref} \left(\frac{T}{Tref} \right)^3 \exp\left[\delta \left(\frac{E_{g,ref}}{T_{ref}} - \frac{E_g}{T} \right) \right] \tag{3}$$

$$E_g = E_{g,ref}\left[1.0 - 0.000268\left(T - T_{ref}\right)\right] \tag{4}$$

$$R_s = R_{s,ref}\frac{T}{T_{ref}}\left(1 - \beta\frac{S}{S_{ref}}\right) \tag{5}$$

$$R_{sh} = R_{sh,ref}\frac{S_{ref}}{S\left[1 + \alpha_{I_{sc}}(T - T_{ref})\right]} \tag{6}$$

$$A = \frac{T}{T_{ref}}A_{ref} \tag{7}$$

$$I = \frac{R_{sh}\left(I_{ph} + I_o\right) - U}{R_s + R_{sh}} - \frac{nTK}{qR_s}LambertW(X) \tag{8}$$

$$X = \frac{qR_sR_{sh}I_o}{ATK\left(R_s + R_{sh}\right)}\exp\left(\frac{qR_{sh}\left(R_sI_{ph} + R_sI_o + U\right)}{ATK\left(R_s + R_{sh}\right)}\right) \tag{9}$$

In the above equation, $I_{ph,ref}$, $I_{o,ref}$, $R_{sh,ref}$, $R_{sh,ref}$, and A_{ref} are the corresponding parameter values under STC conditions and can be calculated; E_g is the bandgap energy value of the photovoltaic module, with a typical value of $E_{g,ref}$ being 1.13 eV; α_{Isc} is the short-circuit current temperature coefficient, with the coefficient β typically set to 0.218, and the coefficient δ typically set to $1/K$.

In this paper, the gray wolf optimization algorithm is selected to extract the five parameters of the single diode equivalent circuit model of the photovoltaic module. However, due to certain limitations of the gray wolf optimization algorithm, this paper further improves upon these limitations, and subsequently applies the improved gray wolf optimization algorithm to the parameter extraction process. Based on this, through extensive experiments, the five parameter values under different operating conditions were extracted. Subsequently, the empirical formulas for the five parameters as functions of S and T, i.e., Equations (2) to (7), were revised, ultimately establishing a photovoltaic module mathematical model with high accuracy under any operating conditions.

II. B. Optimization configuration model for photovoltaic intelligent edge terminals

This paper considers both the purchase cost of photovoltaic smart edge terminals and the cost losses caused by reduced reliability, and constructs an optimization configuration model for photovoltaic smart edge terminals with the goal of minimizing total cost.

II. B. 1) Objective Function

1) Equal annual investment cost. The equal annual investment cost of photovoltaic smart edge terminals is:

$$C^1 = C^D(1+\rho)A(r,n) \tag{10}$$

$$C^D = P^T N \tag{11}$$

$$A(r,n) = \frac{r(1+r)^n}{(1+r)^{n-1} - 1} \tag{12}$$

In the formula: C^I is the equivalent annual investment cost; C^D is the cost of purchasing a batch of photovoltaic smart edge terminals; ρ is the ratio of maintenance and operating costs of photovoltaic smart edge terminals to the purchase cost of photovoltaic smart edge terminals; $A(r,n)$ is a factor measuring economic efficiency; r is the discount rate; n is the service life of photovoltaic smart edge terminals; N is the number of photovoltaic smart edge terminals deployed in the region; P^T is the price per unit of photovoltaic smart edge terminal.

2) Cost reduction due to reliability losses. Different distributed photovoltaic power plants have varying capacities, power generation levels, and importance, leading to different losses due to reduced reliability. Therefore, different power plants should be treated differently. This paper uses capacity ratio as the basis for determining importance weights, with a distributed photovoltaic power plant of capacity W^T as the standard, and the ratio of each distributed photovoltaic power plant's capacity to W^T as its importance weight.

The distance loss coefficient k is:

$$k = \frac{W_j}{W^T} \tag{13}$$

In the formula: W^T is the standard capacity; W_j is the capacity of distributed photovoltaic power station j.

The cost C^C caused by reliability loss is:

$$C^{\mathrm{C}} = \lambda L_{uv}^2 k \tag{14}$$

In the formula: λ is a constant coefficient related to cost losses; L_{uv} is the distance between photovoltaic smart edge terminal u and distributed photovoltaic power station v.

In summary, the objective function of this paper is:

$$\min C = C^{\mathrm{C}} + C^{\mathrm{I}} \tag{15}$$

II. B. 2) Constraints

1) Communication connection constraints. Distributed photovoltaic power stations within the region must establish a communication connection with any photovoltaic intelligent edge terminal within the region:

$$\sum_{v=1}^{M} A_{uv} = 1.0 \tag{16}$$

$$A_{uv} = \begin{cases} 1.0 & \text{Connected} \\ 0.0 & \text{Not connected} \end{cases} \tag{17}$$

In the equation: M represents the total number of distributed photovoltaic power stations in the region; u represents the u th photovoltaic intelligent edge terminal in the region; v represents the v th distributed photovoltaic power station in the region; A_{uv} is a 0-1 variable. If the u th PVIET in the region establishes a communication connection with the v th distributed photovoltaic station in the region, then it is 1.0; otherwise, it is 0.0.

2) Initial funding constraints. Due to funding limitations, the cost of purchasing photovoltaic intelligent edge terminals cannot exceed the initial funding C^T.

$$0 \le C^D \le C^T \tag{18}$$

3) Communication distance constraints. The communication distance between photovoltaic smart edge terminals and distributed photovoltaic power stations within various communication areas cannot exceed the maximum communication distance $R_{\max}$. Since the maximum communication distance is related to the type of communication cable, the selection of $R_{\max}$ is influenced by the type of communication cable used.

$$A_{uv} L_{uv} \le R_{\max} \tag{19}$$

4) Communication connection quantity constraint. The number of distributed photovoltaic power stations connected to a single photovoltaic intelligent edge terminal cannot exceed $U_{\max}$.

$$U_u \le U_{\max} \tag{20}$$

In the equation: U_u represents the number of distributed photovoltaic power plants connected to photovoltaic intelligent edge terminal u.

Analyzing the characteristics of the above problem, it is found that when the number of photovoltaic intelligent edge terminals N is already determined, the problem becomes a special assignment problem of assigning N photovoltaic intelligent edge terminals to M distributed photovoltaic power plants. Both assignment problems and unequal assignment problems have mature solutions. However, since the total cost is not only related to the cost losses caused by reduced reliability but also to the procurement cost of photovoltaic intelligent edge terminals, the number of photovoltaic intelligent edge terminals cannot be determined, the optimization layout model has numerous constraints, and there is strong coupling between integers, making it difficult to solve using traditional integer linear programming methods. The gray wolf optimization algorithm is a meta-heuristic optimization algorithm suitable for solving large-scale real-world multimodal, discontinuous, and non-differentiable problems. Therefore, this paper proposes a gray wolf optimization algorithm based on mutation and reverse learning to solve the model.

II. C. Model solution based on the gray wolf optimization algorithm

II. C. 1) Traditional Gray Wolf Algorithm

The gray wolf algorithm simulates the process of a wolf pack searching for prey. The top 3.0 individuals in the population are named α, β, and δ, representing the 3.0 wolves in the leadership class of the gray wolf population; the remaining candidate individuals are named ω. By solving problems through operations such as surrounding prey and hunting, this algorithm has been widely applied in areas such as feature subset selection and multi-input multi-output power systems.

1) Surrounding the prey. After a gray wolf individual confirms its distance from the prey, it predicts the prey's movement and approaches it. This behavior of the wolf pack is referred to as “surrounding the prey,” with the calculation formula being:

$$D = \left| CX_p(n) - X(n) \right| \tag{21}$$

$$X(n+1) = X_p(n) - AD \tag{22}$$

$$A = 2ar_1 - a \tag{23}$$

$$C = 2r_2 \tag{24}$$

In the equation, D represents the distance between a gray wolf and its prey; A and C are parameters; n is the number of iterations; $X_p(n)$ is the prey position in the n th generation; $X(n)$ is the position vector of the gray wolves in the n th generation; a is the convergence coefficient; r_1 and r_2 are random values between 0.0 and 1.0.

2) Hunting. Since the optimal solution position is unknown, it is assumed that the leaders α, β, and δ are closer to the prey. The ω wolf does not need to directly search for the prey but instead moves toward the center value of the three leaders' positions to complete the hunt. The calculation formula is:

$$D_i(n) = \left| C_i X_i(n) - X(n) \right| \tag{25}$$

$$i = \alpha, \beta, \delta \tag{26}$$

$$\begin{cases} X_1(n) = X_\alpha(n) - A_1 D_\alpha(n) \\ X_2(n) = X_\beta(n) - A_2 D_\beta(n) \\ X_3(n) = X_\delta(n) - A_3 D_\delta(n) \end{cases} \tag{27}$$

$$X(n+1) = \frac{X_1(n) + X_2(n) + X_3(n)}{3} \tag{28}$$

In the equation, D_α, D_β, and D_δ represent the distances between α, β, δ, and other individuals, respectively; X_α, X_β, and X_δ represent the current positions of α, β, and δ, respectively.

II. C. 2) Spatial recognition mechanism of the current search solution

The traditional gray wolf algorithm has strong convergence performance, but it ignores the global performance of the objective during the search for feasible solutions and struggles to simultaneously optimize multiple objectives during the optimization process. To address these issues, a spatial recognition mechanism is introduced based on the constraint violation degree of the current search solution, enabling the algorithm to escape the current environment and approach the feasible region. The computational steps are as follows:

1) Set search parameters, including the optimization objective, iteration count, search target, and exit conditions.

2) Randomly select a computational time slot within the scheduling period and determine the constraint violation degree of that time slot. If the constraint violation degree is greater than 0, proceed to step 3; otherwise, proceed to step 4.

3) Based on the constraint violation degree, identify the feasible region of the decision variables in the current time slot using stored information. Drive the decision variables toward the feasible region through spatial identification of the feasible region. The calculation formula is:

$$\begin{cases} X_t = X_t + er_3\left(X_t^{\max} - X_t^{\min}\right) & r_7 \le 0.4 \\ X_{t+1} = X_{t+1} - er_4\left(X_{t+1}^{\max} - X_{t+1}^{\min}\right) & 0.4 < r_7 \le 0.8 \\ X_t = X_t + er_5\left(X_t^{\max} - X_t^{\min}\right) & 0.8 < r_7 \\ X_{t+1} = X_{t+1} - er_6\left(X_{t+1}^{\max} - X_{t+1}^{\min}\right) & 0.8 < r_7 \end{cases} \tag{29}$$

In the formula, $r_1 \sim r_7$ are random values between 0.0 and 1.0, representing the magnitude of change in the decision variables for the current time period; e is the driving parameter, representing the direction of change in the decision variables for the current time period. When the lower limit is violated, e takes the value 1.0, and when the upper limit is violated, it takes the value -1.0.

4) Adjust the decision variable for the current time period based on the constraint violation information from the adjacent time periods to reduce the likelihood of violations occurring in the adjacent time periods due to changes in the decision variable for the current time period. The calculation formula is:

$$X_t = X_t + er_8\left(X_t^{\max} - X_t^{\min}\right) \tag{30}$$

In the equation, r_8 is a random value between 0 and 1. When both the current and previous time periods violate the upper bound, e is set to -1.0; when both violate the lower bound, e is set to 1.0; in all other cases, e is set to 0.0.

5) Repeat steps (2) to (4). After reaching the maximum number of iterations, compare the current search solution with the original solution. If the constraint violation degree of the current search solution is no higher than that of the original solution, it is considered non-inferior to the original solution. If the target power generation is also greater than the original solution, replace it with the current search solution; otherwise, return the original solution.

6) Set $t = 366$ and complete the iterative correction in reverse order of the scheduling cycle. Calculate the upper and lower limits of the reservoir capacity for the previous time period, $X_{t-1}^{\max}$ and $X_{t-1}^{\min}$, and correct X_{t-1} to satisfy the constraints; Set $t = t - 1.0$ and sequentially correct the reservoir capacity for each time period until $t = 1.0$, at which point the scheduling cycle iteration is complete. The correction method is as follows:

$$X_{t-1} = \begin{cases} X_{t-1}^{\max} & X_{t-1} > X_{t-1}^{\max} \\ X_{t-1} & X_{t-1}^{\min} \le X_{t-1} \le X_{t-1}^{\max} \\ X_{t-1}^{\min} & X_{t-1} < X_{t-1}^{\min} \end{cases} \tag{31}$$

III. Practical application of gray wolf optimization algorithm to improve the efficiency of photovoltaic power station components

III. A. Analysis of algorithm optimization effects

III. A. 1) Comparison of algorithm optimization success rates

Set up a simulation experiment to optimize the efficiency and cost of photovoltaic power plant components, and compare its performance with traditional GWO algorithms and particle swarm optimization (PSO) algorithms. By statistically analyzing the results of performance tests for the three algorithms, we compare and analyze their overall performance to validate the effectiveness of the optimized GWO algorithm with the introduction of a spatial recognition mechanism. In the comparative experiments, to ensure a fair comparison, all three algorithms were run with the same experimental parameters: the maximum number of evaluations of the fitness function was set to 20,000 (population size N = 35, maximum iteration count D = 650). The convergence factor decreases linearly from 3.0 to 0.0 as the number of iterations increases. For the five test functions, each of the three algorithms was run independently 35 times, and the average success rate of converging to the optimal solution was recorded. Table 1 shows the comparison of the optimization success rates of the three algorithms. Across different iteration counts for the five test functions, the optimization success rate of the optimized GWO algorithm remained consistently at 100.0%, while the optimization success rates of the other two algorithms did not exceed 99.0%, typically ranging between 96.0% and 99.0%. The optimized GWO algorithm demonstrated a higher and more stable optimization success rate.

Table 1: Comparison of the optimization success rates of 3 algorithms

Function	Algorithm	D=50(%)	D=350(%)	D=650(%)
F1	PSO	98.2	96.1	93.6
	GWO	98.5	97.4	94.7
	Optimize GWO	100.0	100.0	100.0
F2	PSO	98.4	97.1	96.5
	GWO	98.6	97.8	97.4
	Optimize GWO	100.0	100.0	100.0
F3	PSO	98.5	97.9	96.3
	GWO	98.8	98.5	98.1
	Optimize GWO	100.0	100.0	100.0
F4	PSO	97.5	97.3	97.0
	GWO	98.2	97.6	97.5
	Optimize GWO	100.0	100.0	100.0
F5	PSO	97.6	97.4	97.2
	GWO	98.8	98.3	98.0
	Optimize GWO	100.0	100.0	100.0

III. A. 2) Algorithm Optimization Configuration Results

Table 2 shows the optimized configuration results of the three algorithms. After iteration, the final component operating cost of the optimized GWO algorithm is 1.20270×10^4 yuan, which is lower than the 1.34324×10^4 yuan of the PSO algorithm and the 1.27296×10^4 yuan of the GWO algorithm. From a cost perspective, the optimized GWO algorithm achieves better final solution results, capable of identifying the lowest-cost solution.

Table 2: Optimal configuration results

Algorithm	NPV	Qmax/m3	PNPV/kW	Q0/m3	Cost/104 yuan
PSO	801	19587	3	0.8Qmax	1.34324
GWO	794	17842	2	0.8Qmax	1.27296
Optimize GWO	327	10093	1	0.8Qmax	1.20270

III. A. 3) Algorithm Convergence Curve

Figure 3 shows the iteration process of the three algorithms. Under the premise of finding the optimal solution, the optimized GWO algorithm only required 118 iterations, which is less than the 378 iterations of the PSO algorithm and the 370 iterations of the GWO algorithm. When obtaining a better solution, the optimized GWO algorithm is faster and more stable, demonstrating obvious performance advantages.

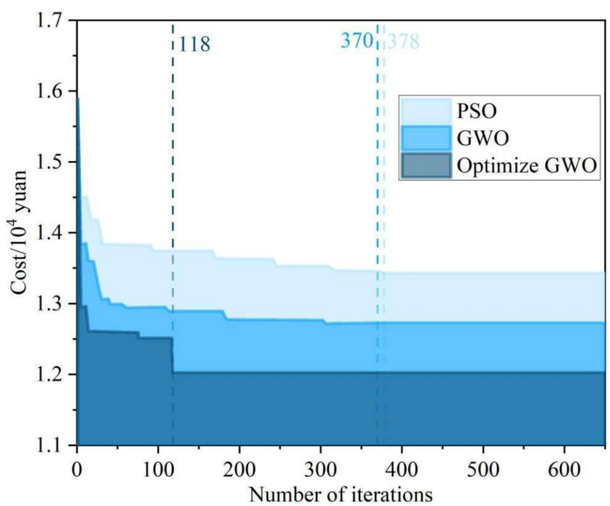

Figure 3: The iterative situations in the solution processes of the three algorithms

III. B. Analysis of power generation efficiency before and after optimization

III. B. 1) Comparison of power generation efficiency before and after optimization

Based on the optimal solution results, the photovoltaic power plant components were optimized, and the power generation efficiency of the photovoltaic power plant before and after optimization was compared to determine the effectiveness of the optimization. Table 3 shows the comparison of power generation efficiency before and after optimization. The improvement ranges for the eight optimized metrics are between 5.8% and 51.5%, all demonstrating positive optimization effects. Among these, the most significant improvement was in power transmission losses, with an improvement rate of 51.5%. Through algorithmic optimization, power transmission losses can be significantly reduced, thereby enhancing power generation efficiency.

Table 3: Comparison of power generation efficiency before and after optimization

Indicator project	Before optimization	After optimization	Improvement range (%)
Annual power generation/(MW·h)	29742.6	37891.5	27.4
Average power generation efficiency /%	15.3	20.1	31.4
System availability rate /%	91.4	98.7	7.9
Component temperature /℃	56.8	40.7	28.4
Inverter efficiency /%	93.4	98.8	5.8
Power transmission loss /%	6.6	3.2	51.5
Operation and maintenance cost /(ten thousands·a-1)	31.7	18.5	41.6
Investment payback period /a	7.9	6.2	21.5

III. B. 2) Optimization of photovoltaic power plant configuration

To verify the correctness of the obtained optimal solution, all feasible solutions were enumerated using the exhaustive method under various operating conditions, proving that the results obtained by the algorithm are optimal solutions. Taking the parallel reactor under full PV power generation as an example, Figure 4 shows the feasible solutions for the parallel reactor under full PV power generation. When 1950 kvar reactors are paralleled at 20 nodes, the fitness function reaches its minimum value of 463.4, which matches the result obtained by the algorithm, confirming that this point is the optimal solution.

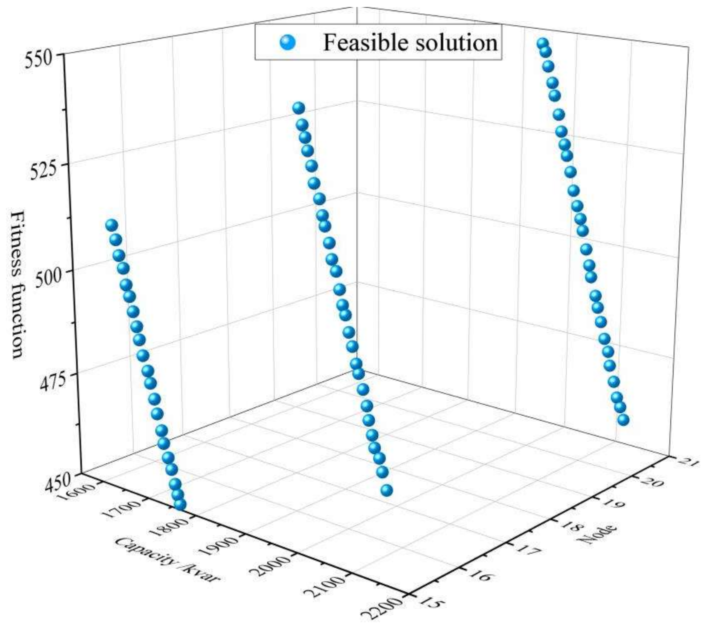

Figure 4: The shunt reactor has a feasible solution

By using the optimal solution as the layout scheme for the two types of components—parallel reactors and series reactors—in a photovoltaic power plant, the optimized system voltage can be obtained. Figure 5 shows the optimized voltage conditions when the photovoltaic system is operating at full capacity. Figure 6 shows the optimized voltage conditions when the photovoltaic system is not operating at full capacity. The optimized voltage for the two types of components when the photovoltaic system is operating at full capacity ranges from 0.94774 V to 1.04615 V, while the optimized voltage for the two types of components when the photovoltaic system is not operating at full capacity ranges from 0.98869 V to 1.04977 V. As can be seen, after optimizing photovoltaic power plant management using the algorithm's solution results, the voltage fluctuation range does not exceed 0.01V under either full or non-full load conditions, with very small fluctuations. This indicates that after optimization, the photovoltaic power plant's module power generation exhibits stability and reliability, with reduced power generation losses and significant improvements in efficiency.

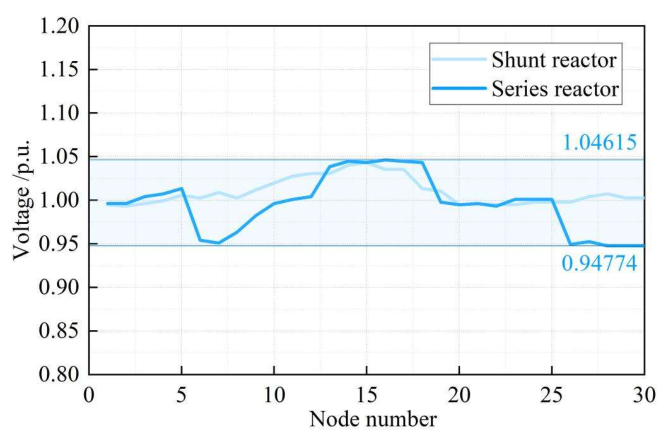

Figure 5: Optimized voltage of photovoltaic power of operating at full capacity

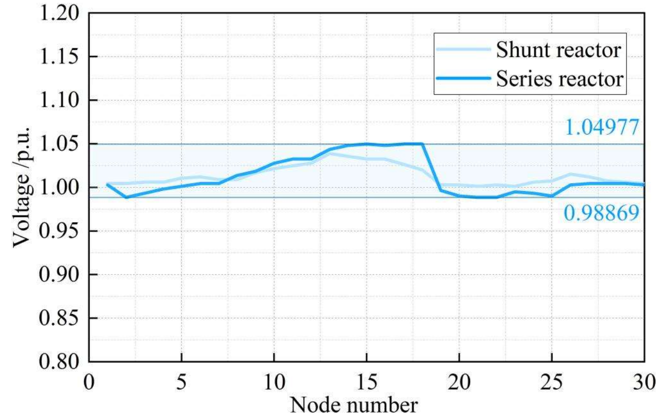

Figure 6: Optimized voltage of the photovoltaic power of not fully generated

IV. Conclusion

This paper utilizes the Gray Wolf Optimization Algorithm to extract and adjust the optimal component parameters of a photovoltaic power plant, thereby enhancing power generation efficiency and stability. Through simulation experiments, the Gray Wolf Optimization Algorithm achieved a 100.0% optimization success rate across all five test functions. The final operational cost was 1.20270×10^4 yuan, outperforming the traditional Gray Wolf Algorithm and Particle Swarm Optimization Algorithm. Additionally, the Gray Wolf Optimization Algorithm required only 118 iterations to obtain the optimal solution, significantly fewer than the 378 and 370 iterations required by the comparison algorithms. After optimizing the photovoltaic power plant components using the solution scheme, the positive improvement range for each power generation project was [5.8, 51.5]%, and the voltage fluctuation of the components under two different operating conditions was less than 0.01V, achieving the goal of the lowest total cost under efficient component operation. In future research, it is possible to explore the introduction of a real-time parameter extraction mechanism to investigate the feasibility of dynamic parameter adjustments, enabling instantaneous response of component parameters and rapid adjustments in photovoltaic power generation.

References

[1] Hayat, M. B., Ali, D., Monyake, K. C., Alagha, L., & Ahmed, N. (2019). Solar energy—A look into power generation, challenges, and a solar‐powered future. International journal of energy research, 43(3), 1049-1067.

[2] Piano, S. L., & Mayumi, K. (2017). Toward an integrated assessment of the performance of photovoltaic power stations for electricity generation. Applied Energy, 186, 167-174.

[3] Zidane, T. E. K., Aziz, A. S., Zahraoui, Y., Kotb, H., AboRas, K. M., & Jember, Y. B. (2023). Grid-connected Solar PV power plants optimization: A review. IEEE Access, 11, 79588-79608.

[4] Hosenuzzaman, M., Rahim, N. A., Selvaraj, J., Hasanuzzaman, M., Malek, A. A., & Nahar, A. (2015). Global prospects, progress, policies, and environmental impact of solar photovoltaic power generation. Renewable and sustainable energy reviews, 41, 284-297.

[5] Alhuwaishel, F. M., Allehyani, A. K., Al-Obaidi, S. A. S., & Enjeti, P. N. (2019). A medium-voltage DC-collection grid for large-scale PV power plants with interleaved modular multilevel converter. IEEE Journal of Emerging and Selected Topics in Power Electronics, 8(4), 3434-3443.

[6] Kafui, A. D., Seres, I., & Farkas, I. (2019). Efficiency comparison of different photovoltaic modules. Acta Technologica Agriculturae, 22(1), 5-11.

[7] Buerhop, C., Bommes, L., Schlipf, J., Pickel, T., Fladung, A., & Peters, I. M. (2022). Infrared imaging of photovoltaic modules: a review of the state of the art and future challenges facing gigawatt photovoltaic power stations. Progress in Energy, 4(4), 042010.

[8] Shukla, A., Kant, K., Sharma, A., & Biwole, P. H. (2017). Cooling methodologies of photovoltaic module for enhancing electrical efficiency: A review. Solar Energy Materials and Solar Cells, 160, 275-286.

[9] Wang, X., & Barnett, A. (2019). The evolving value of photovoltaic module efficiency. Applied Sciences, 9(6), 1227.

[10] Akinyele, D. O., Rayudu, R. K., & Nair, N. K. C. (2015). Global progress in photovoltaic technologies and the scenario of development of solar panel plant and module performance estimation− Application in Nigeria. Renewable and Sustainable Energy Reviews, 48, 112-139.

[11] Vodapally, S. N., & Ali, M. H. (2022). A comprehensive review of solar photovoltaic (PV) technologies, architecture, and its applications to improved efficiency. Energies, 16(1), 319.

[12] Beránek, V., Olšan, T., Libra, M., Poulek, V., Sedláček, J., Dang, M. Q., & Tyukhov, I. I. (2018). New monitoring system for photovoltaic power plants' management. Energies, 11(10), 2495.

[13] Rediske, G., Michels, L., Cezar Mairesse Siluk, J., Donaduzzi Rigo, P., Brum Rosa, C., & Jochann Franceschi Bortolini, R. (2022). Management of operation and maintenance practices in photovoltaic plants: Key performance indicators. International Journal of Energy Research, 46(6), 7118-7136.

[14] Al Smadi, T., Handam, A., Gaeid, K. S., Al-Smadi, A., Al-Husban, Y., & smadi Khalid, A. (2024). Artificial intelligent control of energy management PV system. Results in Control and Optimization, 14, 100343.

[15] Giglio, E., Luzzani, G., Terranova, V., Trivigno, G., Niccolai, A., & Grimaccia, F. (2023). An efficient artificial intelligence energy management system for urban building integrating photovoltaic and storage. IEEE Access, 11, 18673-18688.

[16] Di Piazza, M. C., Pucci, M., & Vitale, G. (2013). Intelligent power conversion system management for photovoltaic generation. Sustainable Energy Technologies and Assessments, 2, 19-30.

[17] Kucęba, R., & Chmielarz, G. (2020, November). Experimental Model of the System for Intelligent Power Plant Management. In 2020 16th International Conference on Network and Service Management (CNSM) (pp. 1-5). IEEE.

[18] Zhang, P., Peng, H., & Xiong, K. (2025). Research and practice on the intelligent photovoltaic power station in Yalong River Basin. Journal of Intelligent Construction.

[19] Boum, A. T., Foba Kakeu, V. J., Mbey, C. F., & Yem Souhe, F. G. (2022). Photovoltaic power generation forecasting using a novel hybrid intelligent model in smart grid. Computational Intelligence and Neuroscience, 2022(1), 7495548.

[20] Rajagopal, V., Sharath, D., Vishwas, G., Bangarraju, J., Arya, S. R., & Venkatesh, C. (2022). Optimized controller gains using grey wolf algorithm for grid tied solar power generation with improved dynamics and power quality. Chinese Journal of Electrical Engineering, 8(2), 75-85.

[21] Aguila-Leon, J., Vargas-Salgado, C., Chiñas-Palacios, C., & Díaz-Bello, D. (2023). Solar photovoltaic Maximum Power Point Tracking controller optimization using Grey Wolf Optimizer: A performance comparison between bio-inspired and traditional algorithms. Expert Systems with Applications, 211, 118700.

[22] Kraiem, H., Aymen, F., Yahya, L., Triviño, A., Alharthi, M., & Ghoneim, S. S. (2021). A comparison between particle swarm and grey wolf optimization algorithms for improving the battery autonomy in a photovoltaic system. Applied Sciences, 11(16), 7732.

[23] Kumar, A., Rizwan, M., Nangia, U., & Alaraj, M. (2021). Grey wolf optimizer-based array reconfiguration to enhance power production from solar photovoltaic plants under different scenarios. Sustainability, 13(24), 13627.

[24] Kingsley-Amaehule, M., Uhunmwangho, R., Nwazor, N., & Okedu, K. E. (2022). Smart intelligent monitoring and maintenance management of photo-voltaic systems. International Journal of Smart Grid, 6(4), 110-122.

[25] Wan, C., Zhao, J., Song, Y., Xu, Z., Lin, J., & Hu, Z. (2015). Photovoltaic and solar power forecasting for smart grid energy management. CSEE Journal of power and energy systems, 1(4), 38-46.

[26] Qiao, X., Guo, D., Li, Y., Xu, Q., Gong, B., Fu, Y., ... & Zhu, D. (2022, December). Photovoltaic Panel Intelligent Management and Identification Detection System Based on YOLOv5. In International Conference on Machine Learning for Cyber Security (pp. 595-606). Cham: Springer Nature Switzerland.

[27] Zhang, X., Ni, L., Zhu, H., Shen, J., & Wang, L. (2024, May). Research on intelligent operation and maintenance system of distributed photovoltaic power station based on Internet of Things technology. In Proceedings of the 2024 International Conference on Generative Artificial Intelligence and Information Security (pp. 380-387).

[28] Aghaei, M., Kolahi, M., Nedaei, A., Venkatesh, N. S., Esmailifar, S. M., Moradi Sizkouhi, A. M., ... & Rüther, R. (2025). Autonomous Intelligent Monitoring of Photovoltaic Systems: An In‐Depth Multidisciplinary Review. Progress in Photovoltaics: Research and Applications, 33(3), 381-409.

[29] Rahman, M. M., Hasanuzzaman, M., & Rahim, N. A. (2015). Effects of various parameters on PV-module power and efficiency. Energy Conversion and Management, 103, 348-358.

[30] Hwang, M. H., Kim, Y. G., Lee, H. S., Kim, Y. D., & Cha, H. R. (2021). A study on the improvement of efficiency by detection solar module faults in deteriorated photovoltaic power plants. Applied Sciences, 11(2), 727.

[31] Zidane, T. E. K., Adzman, M. R. B., Tajuddin, M. F. N., Zali, S. M., & Durusu, A. (2019). Optimal configuration of photovoltaic power plant using grey wolf optimizer: A comparative analysis considering CdTe and c-Si PV modules. Solar Energy, 188, 247-257.

[32] Huang, K. H., Chao, K. H., Kuo, Y. P., & Chen, H. H. (2023). Maximum power point tracking of photovoltaic module arrays based on a modified gray wolf optimization algorithm. Energies, 16(11), 4329.

[33] Ge, L., Liu, J., Wang, B., Zhou, Y., Yan, J., & Wang, M. (2021). Improved adaptive gray wolf genetic algorithm for photovoltaic intelligent edge terminal optimal configuration. Computers and Electrical Engineering, 95, 107394.